

## INVESTIGATION ON EFFECT OF TIG WELDING PARAMETERS ON DISSIMILAR WELD JOINTS OF AISI 304 AND AISI 310 STEELS USING RESPONSE SURFACE METHOD

Rami Reddy PADALA V.<sup>1,\*</sup>, Kesava RAO V. V. S.<sup>2</sup>

### ABSTRACT

Dissimilar weld joints play a major role in power generation, electronic, nuclear reactors, petrochemical and chemical industries due to environmental concerns, energy saving, high performance, cost saving and so on. However efficient welding of dissimilar metals has posed a major challenge due to difference in thermal, mechanical and chemical properties of the materials to be joined under a common welding condition. In the present work dissimilar joints of AISI 304 and AISI 310 steels are produced using Tungsten Inert Gas (TIG) welding. Welding current, wire feed rate, flow rate of gas and edge included angle are considered as input parameters and tensile strength, Impact strength and Maximum bending load are considered as output responses. Response Surface Method (RSM) is adopted using Central Composite Design (CCD) and 31 experiments were performed for 4 factors and 5 levels. Tensile strength, impact strength and maximum bending load are measured. Analysis of Variance (ANOVA) is carried out at 95% confidence level. Effect of welding parameters on output responses are studied by drawing main effect plots, contour plots and surface plots. Optimal weld parameters are identified using Response optimizer

**Keywords:** Dissimilar welds, AISI 304, AISI 310, steels, TIG welding

### INTRODUCTION

In Welding is a joining process in which we can make permanent joint at contacting surfaces of metals, alloys or plastics by application of heat and or pressure. In welding, the work-pieces are melted at the interface and after solidification a permanent joint at interface can be achieved. In some welding a filler material is added for forming weld pool of molten material, which after solidification provides a strong bond between the materials. The ability of a material to be welded is known as weldability of a material and it depends on different factors like melting point of metal, thermal conductivity, reactivity of material with surrounding, material's coefficient of thermal expansion etc.

### Metallurgy of a welded joint

Metal is heated over the range of temperature up to fusion and followed by cooling ambient temperature. Due to differential heating, the material away from the weld bead will be hot but as the weld bead is approached progressively higher temperatures are obtained, resulting in a complex micro structure. The subsequent heating and cooling results in setting up internal stresses and plastic strain in the weld.

A joint produced without a filler metal is called autogenously and its weld zone is composed of re-solidified base metal. A joint made with a filler metal is called weld metal. Since central portion of the weld bead will be cooled slowly, long columnar grains will developed and in the out ward direction grains will become finer and finer with distance.

So the ductility and toughness decreases away from the weld bead. However strength increases with the distance from the weld bead. The original structure in steels consisting of ferrite and pearlite is changed to alpha iron. The weld metal in the molten state has a good tendency to dissolve gases which come into contact with it like oxygen, nitrogen and hydrogen.

So during solidification, a portion of these gases get trapped into the bead called porosity. Porosity is responsible for decrease in the strength of the weld joint. Cooling rates can be controlled by preheating of the base metal welding interface before welding. The heat affected zone is within the base metal itself. It has a microstructure different from that of the base metal after welding, because it is subjected to elevated temperature for a substantial

*This paper was recommended for publication in revised form by Regional Editor Ayşegül Akdoğan Eker*

<sup>1</sup> *Research Scholar, Department of Mechanical Engineering, Andhra University, Visakhapatnam, India*

<sup>2</sup> *Professor, Department of Mechanical Engineering, Andhra University, Visakhapatnam, India*

*\* E-mail address: reddy.pvr2009@gmail.com*

*Orcid id: <https://orcid.org/0000-0002-0905-9688>*

*Manuscript Received 18 April 2020, Accepted 23 December 2020*

period of time during welding. In the heat affected zone, the heat applied during welding recrystallizes the elongated grains of the base metal, grains that are away from the weld metal will recrystallizes into fine equiaxed grains.

### **Dissimilar welding**

Joining of dissimilar metals has found its use extensively in power generation, electronic, nuclear reactors, petrochemical and chemical industries mainly to get tailor made properties in a component and reduction in weight. However efficient welding of dissimilar metals has posed a major challenge due to difference in thermo-mechanical and chemical properties of the materials to be joined under a common welding condition. This causes a steep gradient of the thermo-mechanical properties along the weld.

A variety of problems come up in dissimilar welding like cracking, large weld residual stresses, migration of atoms during welding causing stress concentration on one side of the weld, compressive and tensile thermal stresses, stress corrosion cracking, etc. Now before discussing these problems coming up during dissimilar welding, the passages coming below throw some light on some of the causes of these problems.

In dissimilar welds, weldability is determined by crystal structure, atomic diameter and compositional solubility of the parent metals in the solid and liquid states. Diffusion in the weld pool often results in the formation of intermetallic phases, the majority of which are hard and brittle and are thus detrimental to the mechanical strength and ductility of the joint.

The thermal expansion coefficient and thermal conductivity of the materials being joined are different, which causes large misfit strains and consequently the residual stresses results in cracking during solidification.

Atul Kumar et al.[1] studied the strength of the welds of SS202 and SS410 stainless steel of 3mm thick using Taguchi Method. Welding current, gas pressure and weld rate are considered as input welding parameters. Iqbaljeet Singh Grewal et al.[2] studied tensile strength and impact toughness of the welded joints using Taguchi method using Welding current, gas flow rate and filler metal are considered in their study. Owunna1 and A. E.Ikpe [3] investigated Ultimate Tensile Strength, modulus of elasticity ,elongation and strain for twenty samples of AISI 4130 Low carbon steel plate. Mukesh Hemnani et al. [4] carried out bead on bar welds on EN8 & EN24 solid cylindrical bar using Tungsten Inert Gas (TIG) welding process. Taguchi method is adopted by considering welding current, welding voltage & gas flow rate as welding parameters K. Nageswara Rao et al. [5] studied a variety of problems come up in dissimilar welding like cracking, large weld residual stresses, migration of atoms during welding causing stress concentration on one side of the weld, compressive and tensile stresses, stress corrosion cracking. Baljeet Singh et al. [6] studied the influence of welding parameters on weld-ability of both stainless steel 304 and mild steel 1018 specimens .Welding voltage, welding speed and gas flow rate are considered. S. Mohan Kumar and N. Siva Shanmugam [7] studied the weldability, mechanical properties and microstructural characterization of activated flux TIG welding of AISI 321 austenitic stainless steel. Effect of Activated Tungsten Inert gas (A-TIG) welding on the surface morphology of type 321 austenitic stainless steel welds are SS compared with conventional TIG welding.

G. Venkatesan et al. [8] studied the effect of ternary fluxes viz. SiO<sub>2</sub>, TiO<sub>2</sub> and Cr<sub>2</sub>O<sub>3</sub> on depth of penetration in A-TIG welding of AISI 409 ferritic stainless steel. Mukesh and Sanjeev Sharma [9] analysed the mechanical properties in austenitic Stainless steel using Gas Tungsten Arc Welding (GTAW) and the influence of different input parameters such as welding current, gas flow rate and welding speed on the mechanical properties during the gas tungsten arc welding of austenitic stainless steel 202 grade. Salah Sabeeh Abed Alkareem [10] compared heat flux generated during welding with and without fillers. The study covered the effect of welding current, welding time, welding velocity, gas flow from cylinder, gas flow before welding and gas flow on the generated heat flux during this comparison.

The objective of the paper is to study the effect of TIG welding parameters on tensile strength, impact strength and maximum bending load of dissimilar joints of AISI 304 and AISI 310 steels.

### **EXPERIMENTATION**

AISI 304 and AISI 310 plates of 5 mm thickness were chosen for welding. First the plates were cut into 100mm x 200mm X 5mm size using shearing machine and cleaned by using Ultrasonic cleaning and further cleaned with PCL 21 cleaner before welding. Copper sinks are fixed to the fixture to minimize weld distortion and extreme care has been taken for proper cutting of plates. Details about weld joint dimensions are shown in Figure 1.

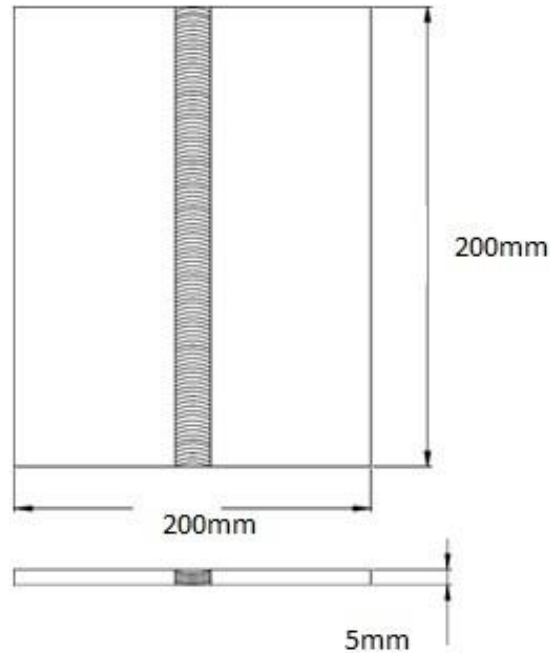


**Figure 1.** Dimensions of welded joint

The chemical composition and tensile properties of AISI 304 and AISI 310 steel plates are given in Table .1 to 4. The welding has been carried out under the welding conditions presented in Table 5. From the earlier works carried out on TIG welding, it was understood that the Welding Current, welding speed, flow rate of gas and edge included angle are the dominating parameters which effect the weld quality characteristics. The range of the welding parameters are chosen based on trial experiments and from earlier works reported [11-16] are presented in Table .6.

Tensile specimens are prepared as per ASTM E8M-04 guidelines using wire cut Electro Discharge Machining in the transverse direction of the weld from each welded sample. Tensile tests are carried out on 100 KN computer controlled Universal Testing Machine (Model No: 8801, INSTRON). The specimen is loaded at a rate of 1.5 KN/min as per ASTM specifications, so that the tensile specimens undergo deformation. From the stress strain curve, the ultimate tensile strength of the weld joints is evaluated and the average of the results of each sample is presented in Table .7. Charpy Impact testing was performed on the weld specimens as per ASTM E23-18. Impact strength per unit volume is measured. Tests were carried out on Three readings are taken for each sample and the average values are reported in Table.7. Bending test is performed as per ASTM E855-08 on the weld samples. Tests were carried out on 1000 Ton capacity TUE-C-1000, FSA (Fine Spavy Associate Pvt Ltd) machine. The maximum bending load is recorded for each weld sample and presented in Table.7.

**Table 1.** Chemical composition of AISI 304 (weight %)

| Element  | Cr    | Mn   | Fe    | Ni   | Cu   | Mo   |
|----------|-------|------|-------|------|------|------|
| Weight % | 18.09 | 1.72 | 71.46 | 7.92 | 0.45 | 0.36 |

**Table 2.** Mechanical properties of AISI 304

| Property | Ultimate Tensile Strength | Yield Tensile Strength | Vickers Hardness |
|----------|---------------------------|------------------------|------------------|
| Value    | 505 MPa                   | 215 MPa                | 210              |

**Table 3.** Chemical composition of AISI 310 (weight %)

| Element  | Cr    | Mn   | Fe    | Ni    | Mo    |
|----------|-------|------|-------|-------|-------|
| Weight % | 25.28 | 0.43 | 53.94 | 20.32 | 0.029 |

**Table 4.** Mechanical properties of AISI 310

| Property | Ultimate Tensile Strength | Yield Tensile Strength | Vickers Hardness |
|----------|---------------------------|------------------------|------------------|
| Value    | 520 MPa                   | 270 MPa                | 225              |

**Table 5.** Welding conditions

|                      |                         |
|----------------------|-------------------------|
| Power source         | ESAB TIG 400i           |
| Polarity             | DCEN                    |
| Mode of operation    | Continuous mode         |
| Filler wire material | AISI 309                |
| Filler wire diameter | 2.4mm                   |
| Welding Gas          | Argon                   |
| Electrode            | Tungsten (2% Thoriated) |
| Electrode Diameter   | 2 mm                    |
| Torch Position       | Vertical                |
| Operation type       | Semi Automatic          |

**Table 6.** Input parameters

| PARAMETER                     | Level |     |     |     |     |
|-------------------------------|-------|-----|-----|-----|-----|
|                               | -2    | -1  | 0   | +1  | +2  |
| Welding Current(Amperes)      | 140   | 150 | 160 | 170 | 180 |
| Gas Flow rate (litres/min)    | 8     | 10  | 12  | 14  | 16  |
| Welding Current (mm/min)      | 120   | 140 | 160 | 180 | 200 |
| Edge Included Angle (Degrees) | 30    | 40  | 50  | 60  | 70  |

### STATISTICAL ANALYSIS

Using MINTAB statistical software design matrix is generated for 4 factors, 5 levels and welding is carried out for all the 31 combination of welding parameters and the values recorded for various tests performed are presented in Table.7

**Table 7.** Experimental values

| Input Parameters |                        |                               |                        |                           | Output Responses       |                          |                         |                        |                          |                         |
|------------------|------------------------|-------------------------------|------------------------|---------------------------|------------------------|--------------------------|-------------------------|------------------------|--------------------------|-------------------------|
| Exp.No.          | Welding Current (Amps) | Flow rate of gas (litres/min) | Welding speed (mm/min) | Edge Included Angle (Deg) | Experimental           |                          |                         | Predicted              |                          |                         |
|                  |                        |                               |                        |                           | Tensile Strength (MPa) | Impact Strength (Joules) | Max. Bending Force (KN) | Tensile Strength (MPa) | Impact Strength (Joules) | Max. Bending Force (KN) |
| 1                | 150                    | 10                            | 140                    | 40                        | 594.13                 | 74                       | 4.6                     | 594.504                | 75                       | 4.6                     |
| 2                | 170                    | 10                            | 140                    | 40                        | 591.08                 | 71                       | 4.6                     | 593.127                | 73                       | 4.6                     |
| 3                | 150                    | 14                            | 140                    | 40                        | 593.42                 | 73                       | 4.7                     | 593.293                | 73                       | 4.7                     |
| 4                | 170                    | 14                            | 140                    | 40                        | 595.13                 | 75                       | 4.5                     | 593.171                | 73                       | 4.5                     |
| 5                | 150                    | 10                            | 180                    | 40                        | 594.25                 | 74                       | 4.6                     | 592.293                | 72                       | 4.6                     |
| 6                | 170                    | 10                            | 180                    | 40                        | 596.46                 | 76                       | 4.7                     | 595.666                | 75                       | 4.7                     |
| 7                | 150                    | 14                            | 180                    | 40                        | 580.79                 | 61                       | 4.5                     | 581.333                | 61                       | 4.5                     |
| 8                | 170                    | 14                            | 180                    | 40                        | 584.75                 | 65                       | 4.4                     | 585.96                 | 66                       | 4.5                     |
| 9                | 150                    | 10                            | 140                    | 60                        | 589.75                 | 70                       | 4.3                     | 588.127                | 68                       | 4.3                     |
| 10               | 170                    | 10                            | 140                    | 60                        | 592.96                 | 73                       | 4.5                     | 590.999                | 71                       | 4.5                     |
| 11               | 150                    | 14                            | 140                    | 60                        | 596.29                 | 76                       | 4.6                     | 595.666                | 76                       | 4.6                     |
| 12               | 170                    | 14                            | 140                    | 60                        | 598.25                 | 78                       | 4.7                     | 599.793                | 80                       | 4.7                     |
| 13               | 150                    | 10                            | 180                    | 60                        | 593.63                 | 74                       | 4.2                     | 594.171                | 74                       | 4.2                     |
| 14               | 170                    | 10                            | 180                    | 60                        | 602.08                 | 80                       | 4.5                     | 601.793                | 81                       | 4.5                     |
| 15               | 150                    | 14                            | 180                    | 60                        | 594.42                 | 74                       | 4.4                     | 591.96                 | 72                       | 4.4                     |
| 16               | 170                    | 14                            | 180                    | 60                        | 602.63                 | 83                       | 4.7                     | 600.838                | 81                       | 4.7                     |
| 17               | 140                    | 12                            | 160                    | 50                        | 590.79                 | 71                       | 4.7                     | 592.541                | 73                       | 4.7                     |
| 18               | 180                    | 12                            | 160                    | 50                        | 599.96                 | 80                       | 4.9                     | 600.041                | 80                       | 4.9                     |
| 19               | 160                    | 8                             | 160                    | 50                        | 592.46                 | 72                       | 4.3                     | 593.374                | 73                       | 4.3                     |
| 20               | 160                    | 16                            | 160                    | 50                        | 590.29                 | 70                       | 4.5                     | 591.208                | 71                       | 4.5                     |
| 21               | 160                    | 12                            | 120                    | 50                        | 590.63                 | 71                       | 4.9                     | 590.879                | 71                       | 4.9                     |
| 22               | 160                    | 12                            | 200                    | 50                        | 588.13                 | 68                       | 4.8                     | 589.713                | 69                       | 4.8                     |
| 23               | 160                    | 12                            | 160                    | 30                        | 590.63                 | 71                       | 4.2                     | 590.046                | 70                       | 4.2                     |
| 24               | 160                    | 12                            | 160                    | 70                        | 596.13                 | 76                       | 4                       | 598.546                | 78                       | 4                       |
| 25               | 160                    | 12                            | 160                    | 50                        | 594.86                 | 75                       | 4.5                     | 595.717                | 76                       | 4.6                     |
| 26               | 160                    | 12                            | 160                    | 50                        | 594.86                 | 75                       | 4.5                     | 595.717                | 76                       | 4.6                     |
| 27               | 160                    | 12                            | 160                    | 50                        | 594.86                 | 75                       | 4.5                     | 595.717                | 76                       | 4.6                     |
| 28               | 160                    | 12                            | 160                    | 50                        | 594.86                 | 75                       | 4.6                     | 595.717                | 76                       | 4.6                     |
| 29               | 160                    | 12                            | 160                    | 50                        | 596.86                 | 77                       | 4.6                     | 595.717                | 76                       | 4.6                     |
| 30               | 160                    | 12                            | 160                    | 50                        | 594.86                 | 75                       | 4.7                     | 595.717                | 76                       | 4.6                     |
| 31               | 160                    | 12                            | 160                    | 50                        | 598.86                 | 78                       | 4.5                     | 595.717                | 76                       | 4.6                     |

**Empirical Mathematical Modelling**

A second order polynomial in some region of the independent variables is employed to develop a relation between the response and the independent variables. If the response is well modeled by a nonlinear function of the independent variables then the approximating function in the second order model is

$$Y = b_0 + \sum b_i x_i + \sum b_{ii} x_i^2 + \sum \sum b_{ij} x_i x_j + \epsilon \tag{1}$$

Where  $b_0, b_i$  are the coefficients of the polynomial and  $\epsilon$  represents noise using MINTAB software by considering the nonlinear model empirical models are developed by considering only the significant coefficients.

$$\begin{aligned} \text{Tensile strength} &= 769.226 - 1.941X_1 + 6.640X_2 + 0.335X_3 - 4.096X_4 - 0.214X_2^2 - 0.003X_3^2 \\ &+ 0.006X_1X_3 + 0.011X_1X_4 - 0.061X_2X_3 + 0.109X_2X_4 + 0.010X_3X_4 \end{aligned} \tag{2}$$

$$\begin{aligned} \text{Impact Strength} &= 244.923 - 1.888X_1 + 4.744X_2 + 0.421X_3 - 3.879X_4 - 0.212X_2^2 - 0.003X_3^2 \\ &+ 0.005X_1X_3 - 0.058X_2X_3 + 0.116X_2X_4 + 0.010X_3X_4 \end{aligned} \tag{3}$$

$$\begin{aligned} \text{Max. Bending Load} = & 26.8091 - 0.2270X_1 + 0.4326X_2 - 0.0733X_3 - 0.0430X_4 + 0.0006X_1^2 \\ & - 0.0101X_2^2 + 0.0002X_3^2 - 0.0012X_4^2 + 0.0016X_1X_2 \\ & + 0.0002X_1X_3 + 0.0007X_1X_4 - 0.0008X_2X_4 + 0.0041X_3X_4 \end{aligned} \quad (4)$$

where  $X_1, X_2, X_3, X_4$  represents the coded values of welding current, gas flow rate, welding speed and edge included angle.

### Analysis of Variance (ANOVA)

The adequacy of the developed models is tested using the ANOVA. As per this technique, if the calculated value of the  $F_{\text{ratio}}$  of the developed model is less than the standard  $F_{\text{ratio}}$  (F-table value 2.56) value at a desired level of confidence of 95%, then the model is said to be adequate within the confidence limit. ANOVA test results are presented in Table .8 for tensile strength, impact strength and maximum bending load. From table 8 it is understood that the developed mathematical models are found to be adequate at 95% confidence level. Coefficient of determination ‘ $R^2$ ’ for the above developed models is found to be above 0.90. The variation of Experimental and predicted values are presented in Scatter plots as shown in figure 2 to 4.

**Table 8.** ANOVA Table

| Tensile strength  |    |         |         |          |       |       |
|-------------------|----|---------|---------|----------|-------|-------|
| Source            | DF | Seq SS  | Adj SS  | Adj MS   | F     | P     |
| Regression        | 14 | 555.60  | 555.60  | 39.686   | 10.30 | 0.000 |
| Linear            | 4  | 201.83  | 86.51   | 21.628   | 5.61  | 0.005 |
| Square            | 4  | 71.80   | 71.80   | 17.949   | 4.66  | 0.011 |
| Interaction       | 6  | 281.97  | 281.97  | 46.995   | 12.20 | 0.000 |
| Residual Error    | 16 | 61.64   | 61.64   | 3.853    |       |       |
| Lack-of-Fit       | 10 | 46.64   | 46.64   | 4.679    | 1.89  | 0.225 |
| Pure Error        | 6  | 14.86   | 14.86   | 2.476    |       |       |
| Total             | 30 | 617.24  |         |          |       |       |
| Impact Strength   |    |         |         |          |       |       |
| Source            | DF | Seq SS  | Adj SS  | Adj MS   | F     | P     |
| Regression        | 14 | 521.64  | 521.64  | 37.260   | 10.37 | 0.000 |
| Linear            | 4  | 184.87  | 73.37   | 19.092   | 5.31  | 0.006 |
| Square            | 4  | 70.85   | 70.85   | 17.714   | 4.93  | 0.009 |
| Interaction       | 6  | 265.91  | 265.91  | 44.319   | 12.34 | 0.000 |
| Residual Error    | 16 | 57.48   | 57.48   | 3.593    |       |       |
| Lack-of-Fit       | 10 | 47.40   | 47.40   | 4.740    | 2.82  | 0.109 |
| Pure Error        | 6  | 10.09   | 10.09   | 1.681    |       |       |
| Total             | 30 | 579.12  |         |          |       |       |
| Max. Bending Load |    |         |         |          |       |       |
| Source            | DF | Seq SS  | Adj SS  | Adj MS   | F     | P     |
| Regression        | 14 | 1.14057 | 1.14057 | 0.081469 | 24.61 | 0.000 |
| Linear            | 4  | 0.15500 | 0.22197 | 0.055494 | 16.76 | 0.000 |
| Square            | 4  | 0.75682 | 0.75682 | 0.189206 | 57.14 | 0.000 |
| Interaction       | 6  | 0.22875 | 0.22875 | 0.038125 | 11.51 | 0.000 |
| Residual Error    | 16 | 0.05298 | 0.05298 | 0.003311 |       |       |
| Lack-of-Fit       | 10 | 0.01583 | 0.01583 | 0.001583 | 0.26  | 0.972 |
| Pure Error        | 6  | 0.03714 | 0.03714 | 0.006190 |       |       |
| Total             | 30 | 1.19355 |         |          |       |       |

where SS= Sum of Squares, MS= Mean Squares, F=Fishers value

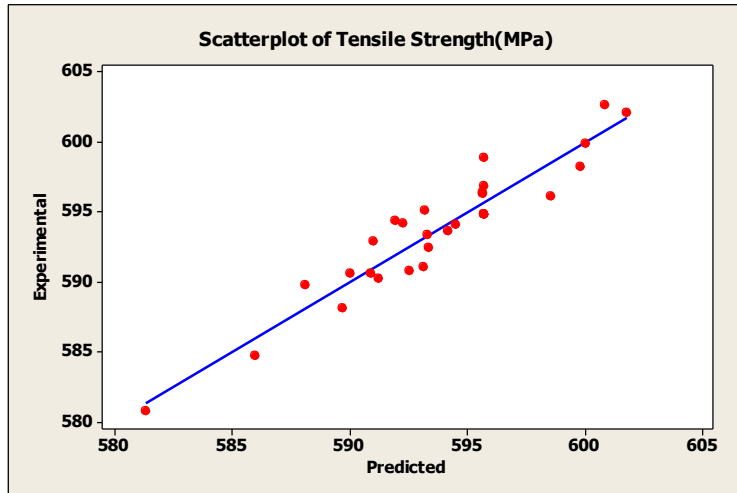


Figure 2. Scatter plot for tensile strength

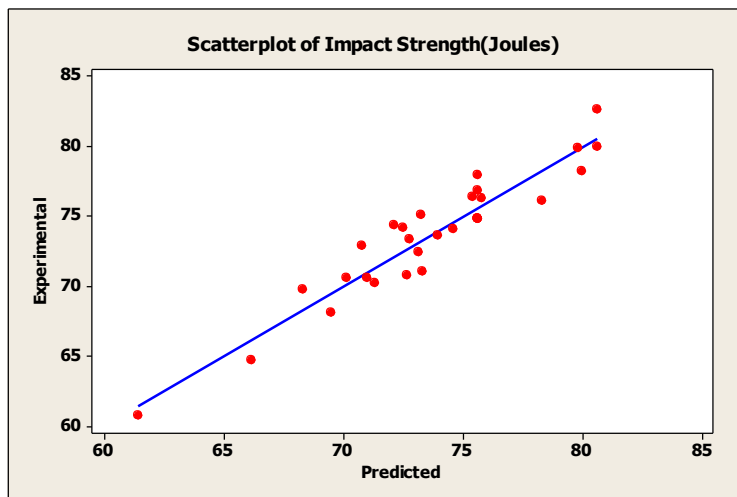


Figure 3. Scatter plot for impact strength

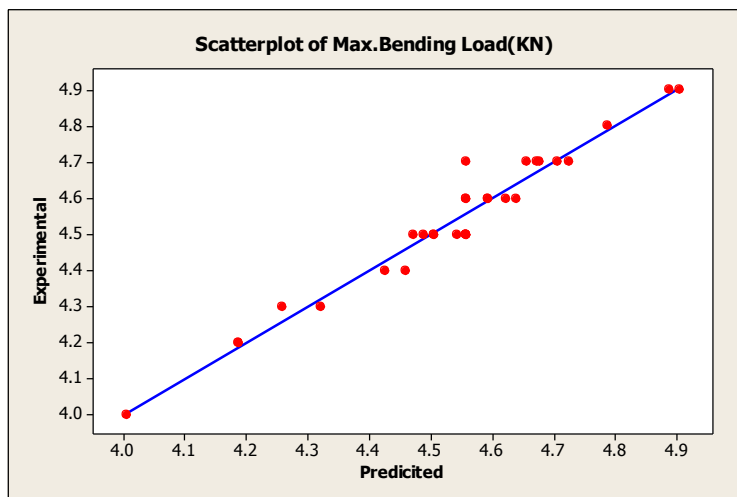
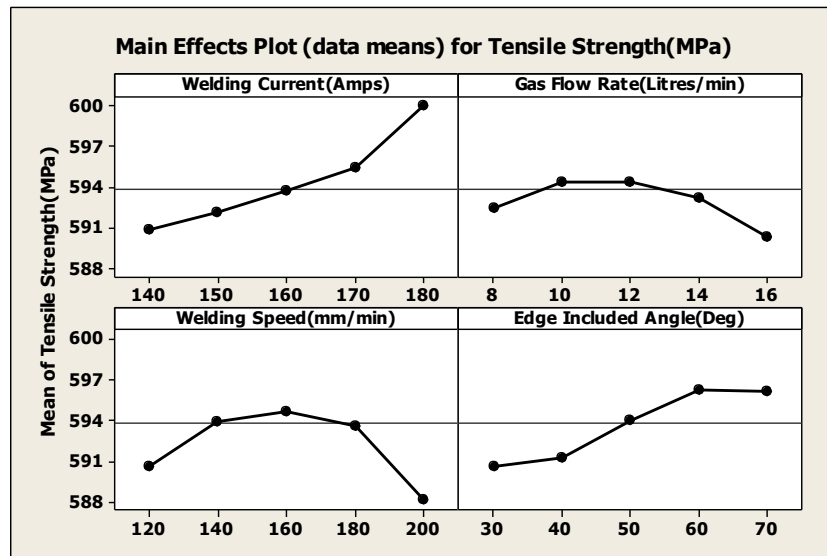


Figure 4. Scatter plot for Max. Bending Load

**Main effect plots**

Main effects of tensile strength, impact strength and maximum bending load are presented in Figure 5, 6 and 7.



**Figure 5.** Main Effects of tensile strength

As welding current increases, heat input increases and the filler metal melts faster leading to faster deposition of filler metal in the weld group leading to higher tensile strength of the welded joint. As flow rate of the welding gas increases the burning capacity increases because of higher amount of gas available, however when the gas flow rate of gas reaches 12 litres/min the filler wire will melt fast and the same time it spills on the outer side of the weld groove leading to poor weld joint and lower tensile strength. Welding speed plays an important role in getting the desired quality. Low welding speeds leads to over melting and higher welding speeds leads to improper penetration. At 160 mm/min optimal welding speed is achieved. While joining thick plate, edge include angle is critical as it decides how much filler material it can accommodate. Higher angle leads to less penetration, whereas lower angle leads to more penetration for same welding speed. Hence optimal edge included angle is important which decides the strength. At edge included angle of 60 Deg optimum tensile strength is obtained.

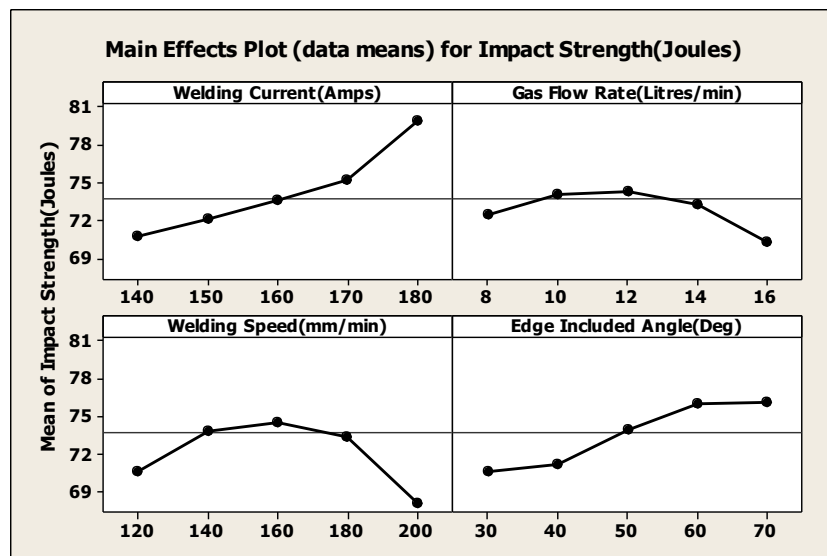


**Figure 6.** Main effects of impact strength



Impact strength of the welded joint improves with welding current because at higher current more heat, which helps in faster melting of filler wire and high deposition rate. Flow rate of welding gas has negative impact on impact strength. Higher flow rates may create blow holes and other defects, which decreases the impact strength. Impact strength improves with welding speed up to 160 mm/min and there after it decreased, this may be due to improper penetration of filler metal. While joining thick plate, edge include angle is critical as it decides how much filler material it can accommodate. Higher angle leads to less penetration, whereas lower angle leads to higher penetration. Hence optimal edge included angle is important which decides the strength. At 60 Deg angle maximum impact strength is noticed, there after the strength remained constant.

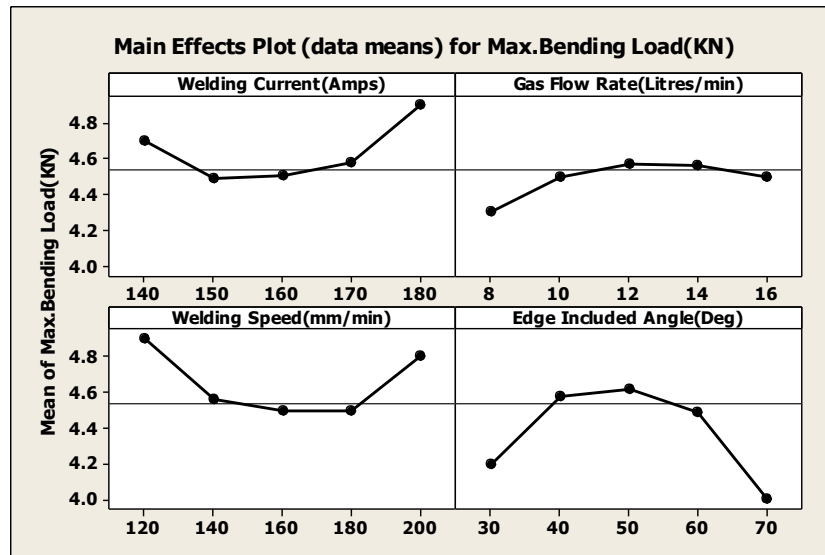


Figure 7. Main effects of Max. Bending Load

Bending load is minimum at welding current of 160 Amps, there after it increased, this may be due to proper fusion of filler metal at higher heat input because of high current. Gas flow rate along with high welding current improves the deposition rate of the filler metal, hence higher bending load. However beyond 12 litres/min, bending load tends to decrease because of violent agitation of molten metal. Bending load decreased with welding speed up to 160 mm/min and there after it increased. The increase in bending load is due to higher penetration of filler metal. Higher Bending load was observed at edge include angle of 50 Deg and there after it decreased, this may be due to incomplete penetration of filler metal because of wider angle.

### Contour plots

The simultaneous effect of two parameters at a time on the output response is generally studied using contour plots. Contour plots play a very important role in the study of the response surface. By generating contour plots using statistical software (MINITAB 14) for response surface analysis, the most influencing parameter can be identified based on the orientation of contour lines. If the contour patterning of circular shaped occurs, it suggests the equal influence of both the factors; while elliptical contours indicate the interaction of the factors. Figure 8 to 10 represents the contour plots for tensile strength, impact strength and maximum bending load.

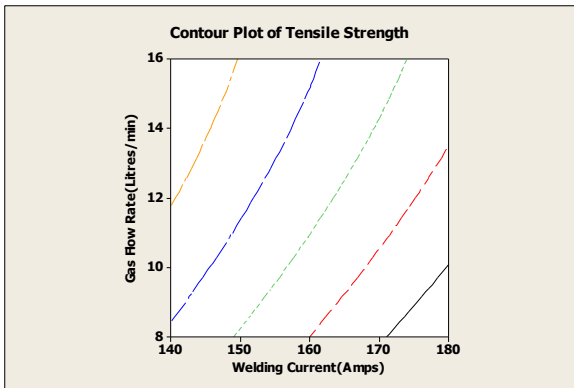


Figure 8(a).

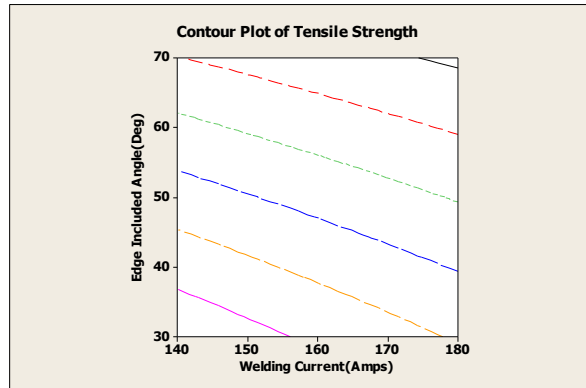


Figure 8(b).

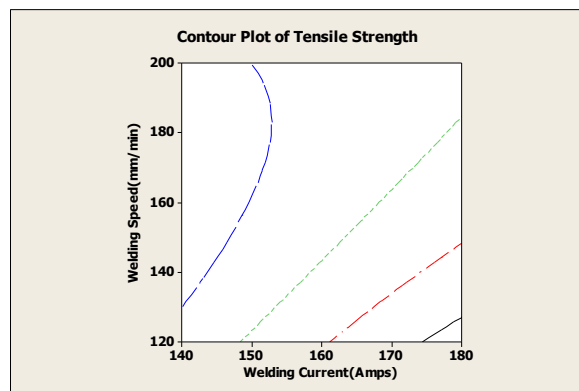


Figure 8(c).

Figure 8. Contour plots for tensile strength

From Fig.8(a) it is clear that welding current is dominating over gas flow rate.  
From Fig.8(b) it is clear that welding current is dominating over edge included angle.  
From Fig.8(c) it is clear that welding current is dominating over welding speed.

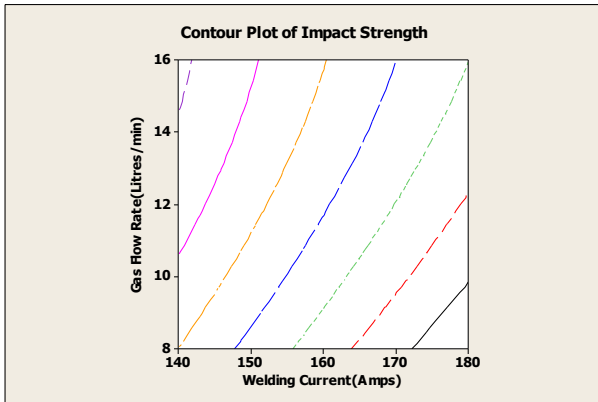


Figure 9 (a).

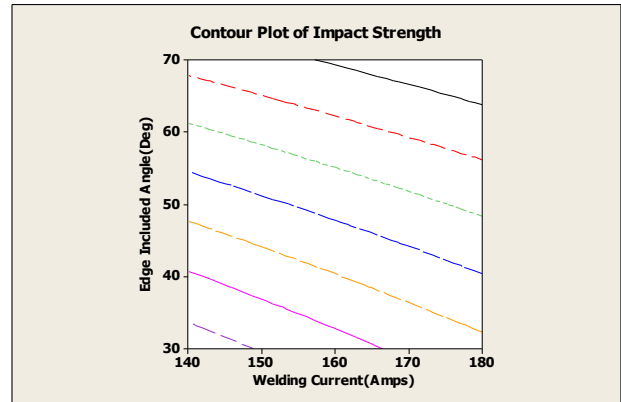


Figure 9(b).

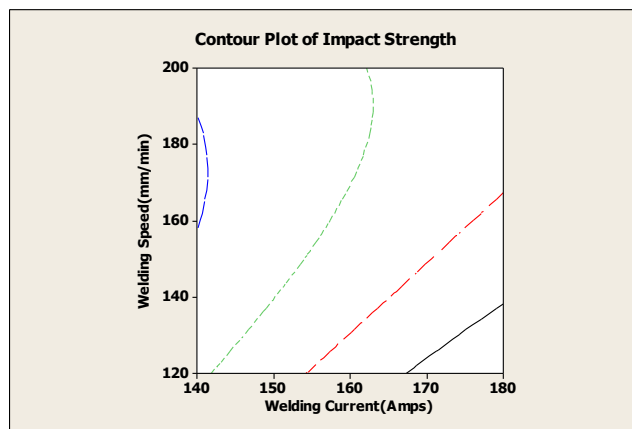


Figure 9 (c).

Figure 9. Contour plots for impact strength

From Fig.9(a) it is clear that welding current is dominating over gas flow rate.  
From Fig.9(b) it is clear that welding current is dominating over edge included angle.  
From Fig.9(c) it is clear that welding current is dominating over welding speed.

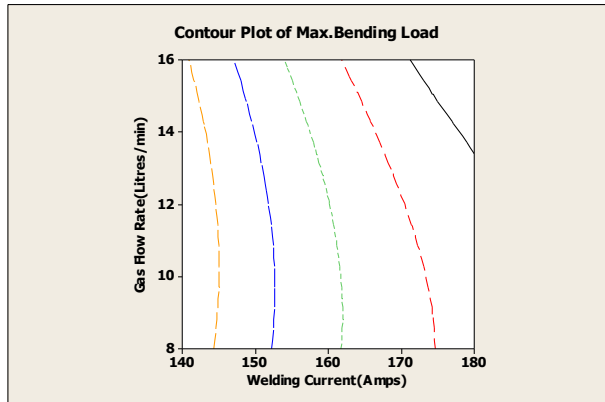


Figure 10(a).

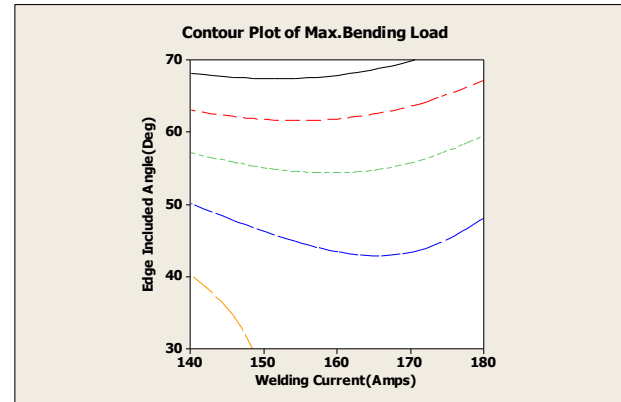


Figure 10(b).

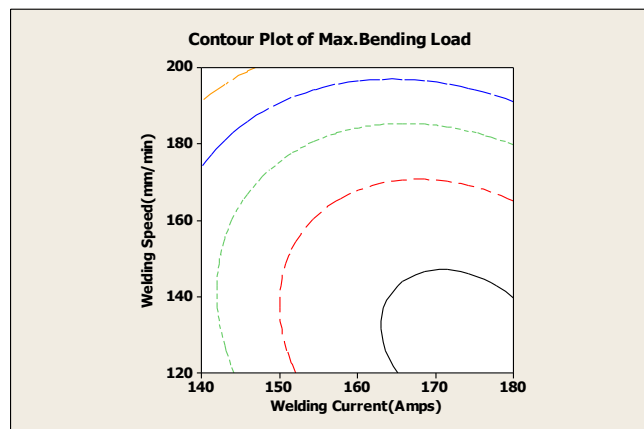


Figure 10(c).

Figure 10. Contour plots for maximum bending load

From Fig.10(a) it is clear that welding current is dominating over gas flow rate.

From Fig.10(b) it is clear that welding current is dominating over edge included angle.

From Fig.10(c) it is clear that welding current is dominating over welding speed.

From the contour plots(Fig.8, 9 and 10), it is understood that the most dominating parameter is welding current, followed by welding speed, flow rate of gas and edge included angle.

### Surface plots

Surface plots are drawn to identify the optimal values of welding parameters. The apex and nadir of the surface plot represent maximum and minimum values of the output response.

Figure 11 to 13 indicates the surface plots for tensile strength, impact strength and Max. Bending load. The objective is to maximize tensile strength, impact strength and Max. Bending load. From the surface plots one can find the optimum value by considering two parameters at a time.

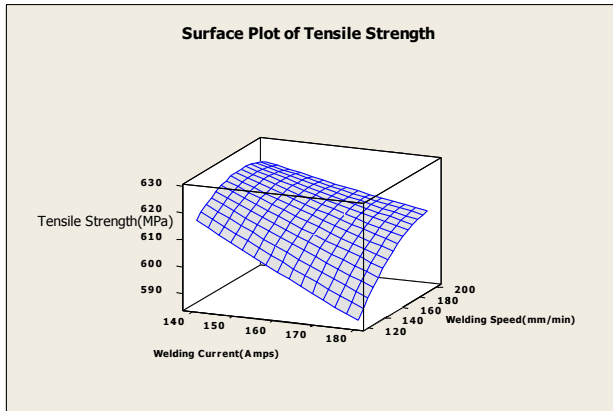


Figure 11(a).

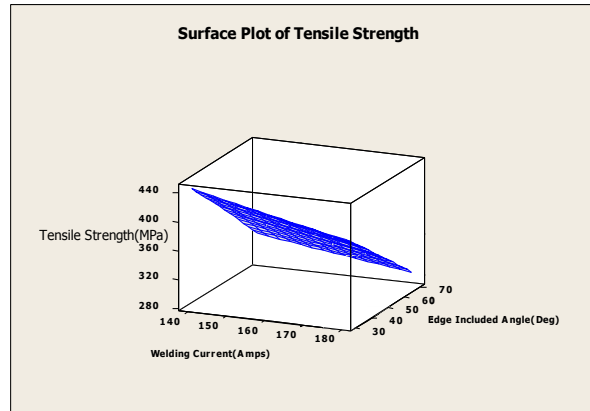


Figure 11(b).

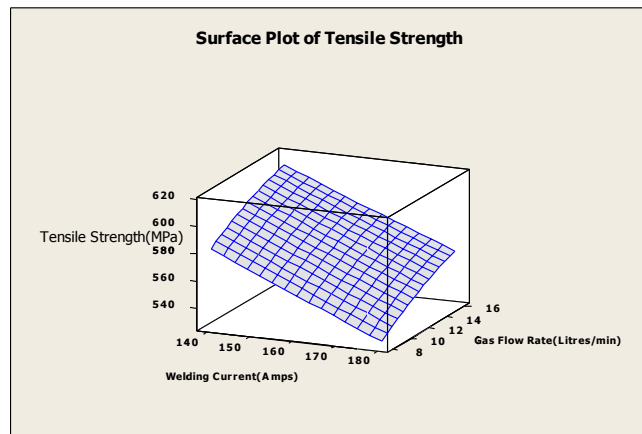


Figure 11 (c).

Figure 11. Surface plots for tensile strength

From Fig.11(a) it is understood that maximum tensile strength is obtained at welding current of 140 Amps and welding speed of 200 mm/min.

From Fig.11(b) it is understood that maximum tensile strength is obtained at welding current of 140 Amps and edge included angle of 60 Deg.

From Fig.11(c) it is understood that maximum tensile strength is obtained at welding current of 140 Amps and gas flow rate of 16 litres/min.

From surface plots of tensile strength (Figure.11), it is understood that maximum tensile strength is obtained at welding current of 140 Amps, gas flow rate of 16 litres/min, welding speed of 200 mm/min and edge included angle of 60 Deg.

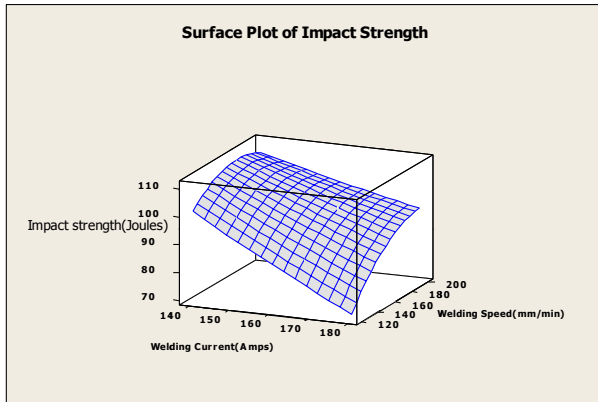


Figure 12(a).

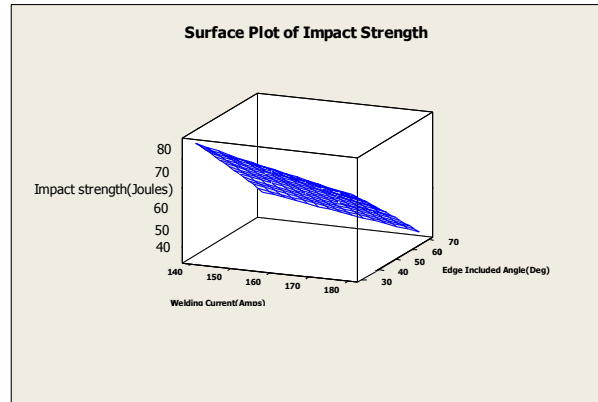


Figure 12(b).

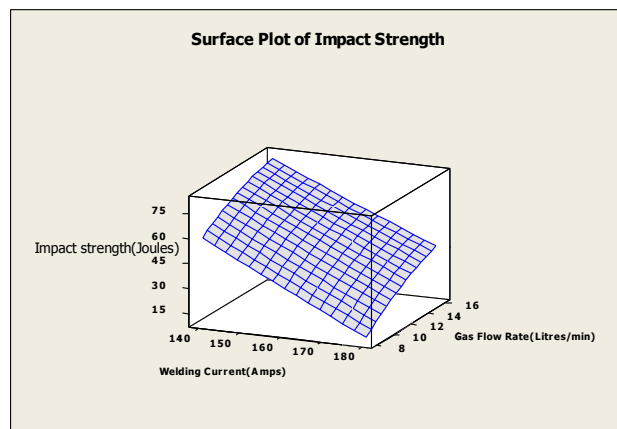


Figure 12(c).

Figure 12. Surface plots for impact strength

From Fig.12(a) it is understood that maximum impact strength is obtained at welding current of 140 Amps and welding speed of 200 mm/min.

From Fig.12(b) it is understood that maximum impact strength is obtained at welding current of 140 Amps and edge included angle of 60 Deg.

From Fig.12(c) it is understood that maximum impact strength is obtained at welding current of 140 Amps and gas flow rate of 16 litres/min.

From surface plots of impact strength (Figure.12), it is understood that maximum impact strength is obtained at welding current of 140 Amps, gas flow rate of 16 litres/min, welding speed of 200 mm/min and edge included angle of 60 Deg

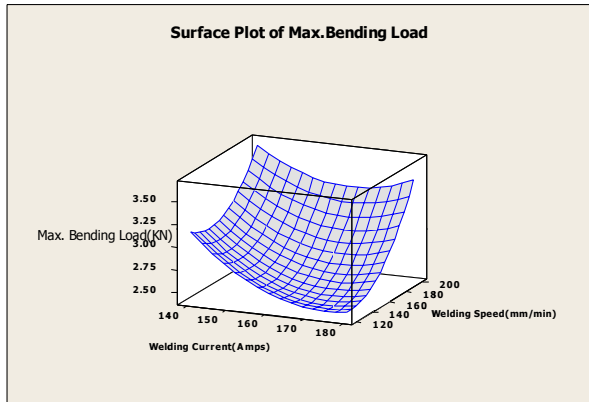


Figure 13(a).

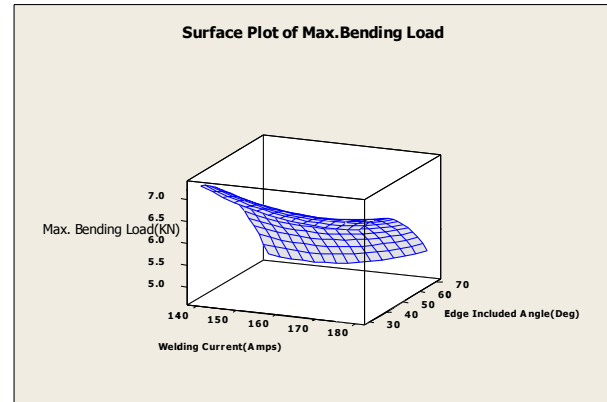


Figure 13(b).

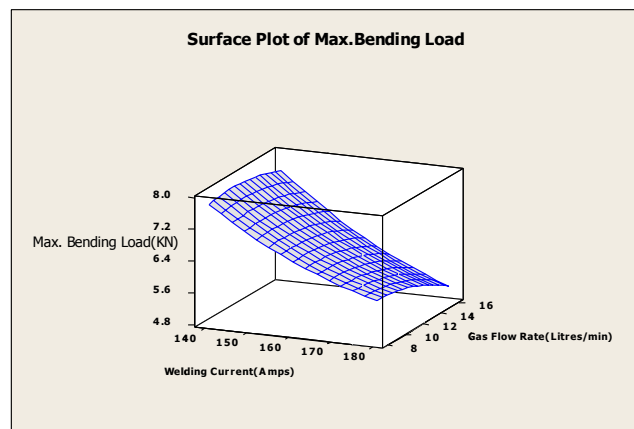


Figure 13(c).

Figure 13. Surface plots for maximum bending load

From Fig.13(a) it is understood that maximum value of Max. Bending load is obtained at welding current of 140 Amps and welding speed of 200 mm/min.

From Fig.13(b) it is understood that maximum value of Max. Bending load is obtained at welding current of 140 Amps and edge included angle of 60 Deg.

From Fig.13(c) it is understood that maximum value of Max. Bending load is obtained at welding current of 140 Amps and gas flow rate of 16 litres/min.

From surface plots of Max. Bending load (Figure.13), it is understood that the maximum value (Max. Bending load) is obtained at welding current of 140 Amps, gas flow rate of 16 litres/min, welding speed of 200 mm/min and edge included angle of 60 Deg.

## OPTIMIZATION

The optimization is carried out using Response optimizer available in MINITAB statistical software. The objective is to maximize tensile strength, impact strength and Max. Bending load. From figure.14 it is understood that at Welding Current of 180 Amps, gas flow rate of 11.6434 litres/min, welding speed of 200 m/min and Edge Include Angle of 63.8392 Deg, optimal Tensile Strength of 609.9863 MPa, Impact Strength of 88.1070 Joules and Max. Bending load of 5.1258 KN are obtained.

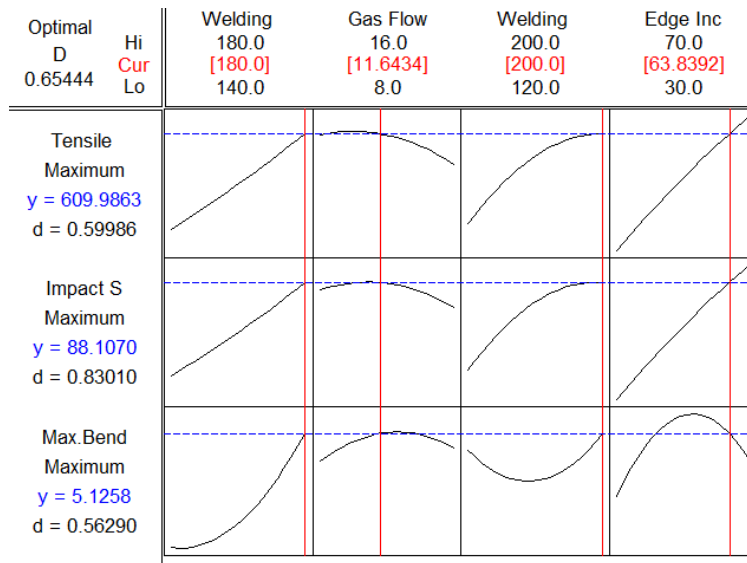


**Figure 14.** Optimal solution of Surface Response Method

Validation experiment is performed, as the optimal welding parameters are not within the 31 experiments presented in Table. Validation experiment is performed at Welding Current of 180 Amps, gas flow rate of 12 litres/min, welding speed of 200 m/min and Edge Include Angle of 64. The measured values of validation experiments are presented in Table.9.

**Table 9.** Validation experiment values

|                         | Optimal value | Experimental value | % error |
|-------------------------|---------------|--------------------|---------|
| Tensile strength (MPa)  | 609.9863      | 602                | 1.32    |
| Impact strength(Joules) | 88.1070       | 84                 | 4.88    |
| Max.Bending Load (KN)   | 5.1258        | 5                  | 2.51    |

## CONCLUSIONS

Based on the experiments performed the following conclusions are drawn:

- 1) Empirical mathematical models are developed for tensile strength, impact strength and maximum bending load for TIG weld dissimilar joints of AISI 304 and AISI 310 using statistical software by considering only the significant coefficients.
- 2) Welding current is the most important parameter which improves the tensile strength, impact strength and maximum bending load; this is due to higher heat input.
- 3) Higher flow rate of welding gas along with welding current increases the melting rate filler wire there by improves the deposition rate.
- 4) Welding speed plays an important role in deposition rate. Low welding speeds lead to over melting and higher welding speeds leads to improper penetration of filler metal.
- 5) Optimal Edge included angle of the weld joint reducing the welding time and improves the weld joint strength.
- 6) From the contour plots, it is observed that the most influencing parameter is welding current, followed by flow rate of gas, fire feed rate and edge included angle.
- 7) From surface plots, we can get optimal combination of two parameters at a time. From overall plots for each output response one may conclude that for maximum tensile strength, impact strength and maximum bending load can be achieved when welding current of 140 Amps, gas flow rate of 16 litres/min, welding speed of 200 mm/min and Edge Include Angle of 60 Deg.
- 8) From Response surface optimizer, it is understood that at Welding Current of 180 Amps, gas flow rate of 11.6434 litres/min, welding speed of 200 mm/min and Edge Include Angle of 63.8392 Deg, optimal Tensile Strength of 609.9863 MPa, Impact Strength of 88.1070 Joules and Max. Bending load of 5.1258 KN are obtained.



## Acknowledgements

The authors thank M/s Metallic Bellows (I), Pvt Ltd, Chennai, IITAM University, Visakhapatnam and GMRIT, Rajam, India for providing the experimental facility.

## REFERENCES

- [1] Atul Kumar, Vikrant Sharma, N. S. Baruaole, Experimental investigation of TIG welding of stainless steel 202 and stainless steel 410 using Taguchi Technique, *International Journal of Computing and Engineering Research*, 1(2), 2017, pp. 98-101.
- [2] Iqbaljeet Singh Grewal, Amrinder Singh, Prabhjot Singh, Experimental Investigation of welding parameters and mechanical properties by Taguchi Method of TIG welded EN 31 Steel and Mild Steel, *International Journal of Engineering Applied Sciences and Technology*, 2(4), 2017, pp. 164-171.
- [3] I Owunna and A. E. Ikpe, Modelling and Prediction of the mechanical properties of TIG welded joint for AISI 4130 low carbon steel plates using Artificial Neural Network (ANN) approach, *Nigerian Journal of Technology*, 38(1), 2019, pp. 117-126.
- [4] Mukesh Hemnani, Promise Mittal, Sachin Goyal, Optimization of Tungsten Inert Gas Welding using Taguchi and ANOVA, *International Journal for Research in Applied Science & Engineering Technology*, 6(V), 2018, pp. 2807-2811.
- [5] K. Nageswararao, B. V. R. Ravi Kumar, M. T. Naik, Study and parameter optimization of dissimilar materials using MIG Welding Process, *International Journal of Engineering and Techniques*, 4(2), 2018, pp. 1081-1085.
- [6] Baljeet Singh, Pankaj Kumar, S. K. Kumara Swamy, Uday Krishna Ravella and Anil Midathda, Microstructure characteristics & mechanical properties of dissimilar TIG weld between Stainless Steel and Mild Steel, *International Journal of Mechanical Engineering and Technology*, 8(7), 2017, pp. 1739-1747. <http://www.iaeme.com/IJMET/issues.asp?JType=IJMET&VType=8&IType=7>.
- [7] S. Mohan Kumar and N. Siva Shanmugam, Studies on the weldability, mechanical properties and microstructural characterization of activated flux TIG welding of AISI 321 Austenitic Stainless Steel, *Materials Research Express*, 2018, pp. 1-58.
- [8] G. Venkatesan, Jimin George, M. Sowmyasri, V. Muthupandi, Effect of ternary fluxes on depth of penetration in A-TIG welding of AISI 409 ferritic stainless steel, *Procedia Materials Science*, 5, 2014, pp. 2402 – 2410.
- [9] Mukesh, Sanjeev Sharma, Study of Mechanical Properties in Austenitic Stainless Steel Using Gas Tungsten Arc Welding (GTAW), *Int. Journal of Engineering Research and Applications*, 3(6), 2013, pp. 547-553.
- [10] Salah Sabeeh Abed Alkareem, An investigation of generated heat flux during welding with and without fillers using different welding conditions, *International Journal of Simulation Systems, Science & Technology*, 20(4), 2019, pp. 1 to 6.
- [11] Mohamed Farid Ben Lamnouar, Mohamed Hadji, Riadbadji, Nabilbensaid, Taharsaadi, Yazid Laibditlaksir, Sabah Senouci, Optimization of TIG welding process parameters for X70-304l dissimilar Joint using Taguchi Method, *Solid State Phenomena*, 297, 2019, pp. 51-61.
- [12] S. C. Juang And Y. S. Tarn, Process parameter selection for optimizing the weld pool geometry in the tungsten inert gas welding of stainless steel, *Journal of Materials Processing Technology*, 122, 2002, pp. 33-37.
- [13] Wichan Chuaiphan, Somrer Chandra-Ambhorn, Satian Niltawach, C. and Banlengornil, Dissimilar Welding between AISI 304 Stainless Steel and AISI 1020 Carbon Steel Plates, *Applied Mechanics and Materials*, 268-270, 2013, pp. 283-290.
- [14] Ajay Kumar, Pradeep Kumar, Srishti Mishra, R. K. Mishraatushar Srivastav, Sachin Mishra Rajeev Kumar, Experimental Process of Tungsten Inert Gas Welding of a Stainless Steel Plate, *Materials Today: Proceedings*, 2, 2015, pp. 3260-3267.
- [15] C. Balaji, S. V. Abinash Kumar, S. Ashwin Kumar, R. Sathish, Evaluation of mechanical properties of SS 316L weldments using Tungsten Inert Gas welding, *International Journal of Engineering Science and Technology*, 4(5), 2012, pp. 2053- 2057.
- [16] Piyush Rana, Baljinder Singh, Jaswant Singh, Parametric Study of Dissimilar Material on Gas Tungsten Arc Welding, *International Journal of Engineering Sciences*, 25, 2017, pp. 60-67.